## eNeuro

Research Article: New Research | Development

### Developmental axon degeneration requires TRPV1-dependent Ca<sup>2+</sup> influx

### Aaron D. Johnstone<sup>1,2</sup>, Andrés de Léon<sup>1,2</sup>, Nicolás Unsain<sup>3</sup>, Julien Gibon<sup>2</sup> and Philip A. Barker<sup>2</sup>

<sup>1</sup>Department of Neurology and Neurosurgery, Montreal Neurological Institute, McGill University, Montreal, Quebec, H3A 2B4, Canada

 <sup>2</sup>Department of Biology, University of British Columbia Okanagan, Kelowna, British Columbia, V1V 1V7, Canada
 <sup>3</sup>Instituto de Investigación Médica Mercedes y Martín Ferreyra, INIMEC-Consejo Nacional de Investigaciones Científicas y Técnicas (CONICET), Universidad Nacional de Córdoba, Córdoba, 5016, Argentina

### https://doi.org/10.1523/ENEURO.0019-19.2019

Received: 15 January 2019

Revised: 23 January 2019

Accepted: 24 January 2019

Published: 1 February 2019

ADJ designed and performed experiments, analyzed data, and wrote the manuscript

ADL designed and performed experiments and analyzed data

NU performed experiments

JG supervised the study and edited the manuscript

PAB supervised the study and edited the manuscript

Funding: Canadian Institute of Health Research MOP137057

**Conflict of Interest:** The authors declare no conflicting interests.

Funding: Canadian Institute of Health Research: Philip Amos Barker MOP137057

Correspondence should be addressed to Philip Barker, philip.barker@ubc.ca

Cite as: eNeuro 2019; 10.1523/ENEURO.0019-19.2019

Alerts: Sign up at www.eneuro.org/alerts to receive customized email alerts when the fully formatted version of this article is published.

Accepted manuscripts are peer-reviewed but have not been through the copyediting, formatting, or proofreading process.

Copyright © 2019 Johnstone et al.

This is an open-access article distributed under the terms of the Creative Commons Attribution 4.0 International license, which permits unrestricted use, distribution and reproduction in any medium provided that the original work is properly attributed.

Developmental axon degeneration requires TRPV1-dependent Ca<sup>2+</sup> influx. Short title: TRPV1 in developmental axon degeneration 7 Aaron D. Johnstone<sup>1,2</sup>, Andrés de Léon<sup>1,2</sup>, Nicolás Unsain<sup>3</sup>, Julien Gibon<sup>2</sup> and Philip A. Barker<sup>2,\*</sup> <sup>1</sup>Department of Neurology and Neurosurgery, Montreal Neurological Institute, McGill University, Montreal, Quebec, H3A 2B4, Canada <sup>2</sup>Department of Biology, University of British Columbia Okanagan, Kelowna, British Columbia, V1V 1V7, Canada <sup>3</sup>Instituto de Investigación Médica Mercedes y Martín Ferreyra, INIMEC-Consejo Nacional de Investigaciones Científicas y Técnicas (CONICET), Universidad Nacional de Córdoba, Córdoba, 5016, Argentina \* Correspondences should be addressed to Philip Barker, FIP322-3247 University Way, Kelowna, British Columbia, Canada, V1V 1V7, philip.barker@ubc.ca Pages: 33 Figures: 6 Abstract: 170 words Significance statement: 118 Introduction: 644 words Discussion: 1266 words Conflict of interest: The authors declare no conflicting interests. Keywords: TRPV1, nerve growth factor, NGF, TrkA, dorsal root ganglion, DRG, calcium, neurodegeneration, developmental degeneration, axon degeneration Author contributions: ADJ designed and performed experiments, analyzed data, and wrote the manuscript ADL designed and performed experiments and analyzed data NU performed experiments JG supervised the study and edited the manuscript PAB supervised the study and edited the manuscript Funding: Canadian Institute of Health Research: Philip Amos Barker MOP137057 

### 47 Abstract

48

49 Development of the nervous system relies on a balance between axon and dendrite growth and 50 subsequent pruning and degeneration. The developmental degeneration of dorsal root ganglion (DRG) sensory axons has been well studied in part because it can be readily modeled by 51 52 removing the trophic support by nerve growth factor (NGF) in vitro. We have recently reported that axonal fragmentation induced by NGF withdrawal is dependent on Ca<sup>2+</sup> and here we address 53 the mechanism of Ca<sup>2+</sup> entry required for developmental axon degeneration of mouse embryonic 54 DRG neurons. Our results show that the Transient Receptor Potential Vanilloid family member 1 55 (TRPV1) cation channel plays a critical role mediating  $Ca^{2+}$  influx in DRG axons withdrawn 56 57 from NGF. We further demonstrate that TRPV1 activation is dependent on reactive oxygen 58 species (ROS) generation that is driven through protein kinase C (PKC) and NADPH oxidase 59 (NOX) -dependent pathways that become active upon NGF withdrawal. These findings demonstrate novel mechanistic links between NGF deprivation, PKC activation, ROS generation 60 and TRPV1-dependent  $Ca^{2+}$  influx in sensory axon degeneration. 61

62

### 63 Significance Statement

Neurons are equipped with the genetic means to degenerate, and a subset of peripheral neurons normally degenerate during embryonic development to establish a mature pattern. This beneficial neurodegeneration is regulated by signaling pathways that are only partially understood, yet share components with pathways that mediate pathological degeneration of crucial neural structures during adult diseases such as Alzheimer's and Parkinson's. Here, we identify TRPV1 as a key regulator of Ca<sup>2+</sup> entry into axoplasm that is required for developmental degeneration modeled by NGF withdrawal from sensory neurons of the dorsal root ganglion *in vitro*. 71 Crucially, we report that the TRPV1-mediated  $Ca^{2+}$  flux is prompted by a signaling axis 72 comprised of PKC-dependent NOX complex activation and ROS generation upstream of 73 TRPV1.

### 75 Introduction

76 Axons normally degenerate during embryonic development to refine the nervous system into its 77 mature pattern (Patel et al., 2000; Schuldiner and Yaron, 2014). In the dorsal root ganglia (DRG), greater numbers of sensory neurons are generated than will persist, and surviving 78 79 neurons are those that arrive at their targets and receive adequate neurotrophic support from a 80 limited pool secreted from their targets (Barde, 1989; Vogelbaum et al., 1998; Saxena and 81 Caroni, 2007). Genetically-encoded components of developmentally-required signaling 82 pathways that mediate the removal of neurites (including tumor necrosis factor receptors 83 (TNFRs), MAP kinases, Bax and caspases) also underlie neurodegenerative diseases such as 84 Alzheimer's, Parkinson's and amyotrophic lateral sclerosis (ALS) when they are dysregulated in 85 adulthood (Kirkland and Franklin, 2003; Fischer and Glass, 2007; Saxena and Caroni, 2007; Vickers et al., 2009; Tait and Green, 2010; Kanaan et al., 2013). 86

87

We recently reported that sensory axons are rescued from developmental degeneration by Ca<sup>2+</sup> 88 89 chelation in vitro (Johnstone et al., 2018). Intriguingly, nerve terminals that innervate the skin can be locally ablated in the clinic by activation of Ca<sup>2+</sup> influx mediated by the cation channel 90 Transient Receptor Potential Vanilloid family member 1 (TRPV1); topical application of the 91 92 TRPV1 agonist capsaicin is used to alleviate chronic pain and itch in humans (Jancso et al., 93 1985; Gibbons et al., 2010; Chiang et al., 2015; Savk, 2016). Since activation of TRPV1 can 94 trigger degeneration in sensory neurons (Wang et al., 2017; Jancso et al., 1985; Sann et al., 1995; Gibbons et al., 2010; Chiang et al., 2015), and because we found that Ca<sup>2+</sup> is required for 95 developmental degeneration (Johnstone et al., 2018), here we have explored the possibility that 96 97 TRPV1 is required for developmental degeneration of sensory axons.

98 TRPV1 was identified through expression cloning designed to find the gene product that 99 mediates Ca<sup>2+</sup> influxes in response to capsaicin (Julius et al., 1997). In the intervening 20 years, 100 TRPV1 has been confirmed to be activated and/or sensitized by heat, protons, reactive oxygen 101 species, by the endogenous compounds N-arachidonoyl dopamine (NADA) and anandamide, by 102 direct oxidation and by an array of noxious pest-defence compounds produced by invertebrates 103 and plants (Hakim et al., 2015; Fenwick et al., 2017; Geron et al., 2017; Grabiec and Dehghani, 104 2017).

105

106 ROS were initially considered a toxic consequence of aerobic respiration, but a large number of 107 studies published in the past two decades have firmly established ROS as second messengers that 108 regulate several signaling cascades (Li et al., 2006, 2009; Bedard and Krause, 2007; Ibi et al., 109 2008; Pal et al., 2013). NADPH oxidase (NOX) complexes are membrane-associated protein 110 complexes that reduce NADPH to generate superoxide from molecular oxygen. The canonical 111 NOX complexes are activated by protein kinase C (PKC), which targets the p47phox subunit for 112 phosphorylation. NOX complexes are major sources of ROS species that regulate survival, 113 plasticity and degeneration (Cox et al., 1985; Maher and Schubert, 2000; Li et al., 2006, 2009; 114 Ibi et al., 2008; Petry et al., 2010; Reczek and Chandel, 2014).

115

116 In this study, we show that axons deprived of NGF display  $Ca^{2+}$  influx prior to fragmentation. 117 This  $Ca^{2+}$  influx was prevented by TRPV1 inhibition or TRPV1 genetic knockout. We 118 hypothesized that ROS are required for TRPV1 activation and the resulting  $Ca^{2+}$  influx, and in 119 support of this, we found that ROS scavengers and NOX complex inhibitors rescue axons from 120  $Ca^{2+}$  influx and fragmentation. PKC activity was necessary for the NGF deprivation-induced

121  $Ca^{2+}$  influx and degeneration that we observed, and direct activation of PKC was sufficient to 122 drive robust  $Ca^{2+}$  influx into axons. We reasoned that PKC, NOX complexes, ROS, TRPV1 and 123  $Ca^{2+}$  comprise a signaling axis in these axons and consistent with this, found that PKC functions 124 upstream of NOX, and ROS to mediate TRPV1-dependent  $Ca^{2+}$  influx. Taken together, these 125 results show that NGF deprivation induces a  $Ca^{2+}$  influx via TRPV1 downstream of PKC and 126 NOX complex-derived ROS during developmental axon degeneration.

### 128 Materials and Methods

### 129 Dissection, culturing and NGF deprivation of DRG explants

130 DRG explants were dissected from pregnant CD1 mice with litters of E13.5 embryos (Charles 131 River). Explants were seeded on 6-well plastic cell culture plates (Greiner) or 4-well glass-132 bottom imaging dishes (CellVis) coated in a three-step process with 1 mg/ml poly-D-lysine 133 (Sigma-Aldrich), 10 µg/ml laminin-entactin complex (Corning) and PurCol bovine collagen 0.1 134 mg/ml (Advanced Biomatrix). Explants were cultured in neurobasal medium (Invitrogen) 135 supplemented with 2% B-27 serum-free supplement (Invitrogen), 1% L-glutamine (Wisent), 1% 136 penicillin/streptomycin (Wisent), and 10 µM 5-fluoro-2'-deoxyuridine (FDU, Sigma-Aldrich) 137 with 12.5 ng/ml NGF (CedarLane). NGF deprivation was achieved using fresh media as described above but lacking NGF and containing 2.8 µg/ml rabbit anti-NGF antibody (produced 138 139 in-house). A full description of the anti-NGF antibody (raised against 2.5s NGF), its specificity 140 and its biological validation in survival and cell-surface binding assays has been published 141 (Murphy et al., 1993). All experimental procedures were approved by the Montreal Neurological 142 Institute Animal Care Committee and University of British Columbia animal care committees 143 and were in compliance with Canadian Council on Animal Care guidelines.

144

145

### 146 Fixation, immunostaining and imaging

DRG cultures were fixed in 4% paraformaldehyde in PBS for 15 minutes at room temperature
and permeabilized and blocked for immunostaining in TBS-T, 5% skim milk, and 0.3% Triton
X-100 for 15 minutes at room temperature. Immunostaining was performed in TBS-T with 5%
skim milk and 0.3% Triton X-100 with mouse anti-β-III tubulin (Millipore; 1:10 000) primary

antibody and anti-mouse secondary antibody conjugated to Alexa Fluor 488 (ThermoFisher; 152 1:5000). Cultures were imaged at 5x magnification using a Zeiss ObserverZ.1 inverted 153 epifluorescence microscope with an automated, motorized stage. Images were stitched 154 automatically with Zen 2 software from Zeiss to produce a master image of all explants on the 155 entire 6-well plate. From this master image, quarter-DRG fields were cropped using NIH ImageJ 156 (FIJI build) to create an image set for quantification as recently described in detail by our group 157 (Johnstone et al., 2018).

158 *Quantification of axon degeneration* 

Axon degeneration was quantified by implementing the R script Axoquant2.0 recently described in detail and made freely available by our group (Johnstone et al., 2018). For plotting and statistical analysis, each point represents the mean value of measurements from the complement of DRG cultured from a single embryo.

163

164  $Ca^{2+}$  chelation

165 After 60h of growth in NGF, cultures were either maintained in NGF or were deprived of NGF 166 and exposed to anti-NGF antibody (2.8  $\mu$ g/ml, produced in-house) in the presence of EDTA 6 167 mM (Sigma-Aldrich) for the final 12 hours or for the entire 24 hours before fixation with 168 paraformaldehyde 4% in PBS, stained as described above and imaged for quantification.

169

### 170 Antioxidant preparation

N-acetylcysteine (NAC, Sigma-Aldrich) was prepared at 20 mM in neurobasal media and pHadjusted to 7.4.

173

### 174 Pharmacological PKC, NOX complex and TRPV1 inhibitors

175 PKC inhibitors Gö6976 and Gö6983, NOX complex inhibitors diphenyliodonium (DPI), 176 apocynin and VAS2870 and TRPV1 inhibitor capsazepine (all obtained from Tocris) were 177 prepared in DMSO and delivered to cultures at 10  $\mu$ M. DMSO did not exceed 0.1% in final 178 culture in any case.

179

### 180 Generation of mixed-genotype TrpV1 embryo litters

181 C57BL6 mice carrying the TRPV1<sup>tm1Jul</sup> (targeted mutation 1, David Julius) knockout allele in 182 homozygosity were obtained from Jackson Laboratories and crossed with wild-type C57BL6 183 mice to generate TRPV1<sup>-/+</sup> animals, and these heterozygotes were bred in timed pregnancies to 184 produce mixed-genotype litters (confirmed by PCR, for primer squences see Table 1) of wild-185 type and *TRPV1<sup>-/-</sup>* E13.5 embryos for DRG isolation.

186

### 187 End-point Ca<sup>2+</sup> imaging with Fluo-4

188 30 minutes prior to imaging, cultures were incubated with 5 µM fluo-4 (Invitrogen) in 189 dimethylsulphoxide (DMSO, Sigma, final concentration in media did not exceed 0.1%) for 15 190 minutes at 37°C and then allowed to equilibrate in fresh, room-temperature HBSS (Wisent) 191 supplemented with 2 mM CaCl<sub>2</sub> for another 15 minutes. Imaging was performed in fresh HBSS 192 with 2 mM CaCl<sub>2</sub> with a Leica DMi8 confocal microscope and LAS X software with a 488 nm 193 laser in 0.3 micrometer z-increments with 63x objective to capture at least two fields of axons 194 per ganglia. Background was corrected from images of sum-z-stacks by averaging the mean 195 pixel intensities within four background regions and subtracting this value from each pixel in the image using ImageJ (FIJI build, NIH). The 2D area occupied by axons in each image was then measured using a binary mask of all axons, and the mean pixel intensity value for each image was divided by the area occupied by axons to provide a measure of fluo-4 fluorescence intensity per unit axon area. Field images of DRG axons from the same embryo were averaged to produce the embryo mean value. In each experiment, measurements were standardized to the NGF control value of 1.0 and the size of the treatment values expressed as fold-change from NGF control.

203

204 *Live*  $Ca^{2+}$  *imaging with fluo-4* 

205 30 minutes prior to imaging, cultures were incubated with 5 µM Fluo-4 (Invitrogen) in 206 dimethylsulphoxide (DMSO, Sigma, final concentration in media did not exceed 0.1%) for 15 207 minutes at 37°C and then allowed to equilibrate at room-temperature, then washed with fresh 208 HBSS (Wisent) supplemented with 2 mM CaCl<sub>2</sub> (Fisher BioReagents) for 15 minutes. Fields of 209 >100 axons each were acquired at 40x at a rate of one frame every 5 seconds on a Zeiss 210 ObserverZ.1 inverted epifluorescence microscope controlled by ZEN2 software with an 211 atmosphere-controlled incubation chamber (Pecon) and 470 nm Colibri LED light source (Zeiss). 212 Before injection of stimulus (PMA 100 nM) baseline fluorescence was recorded for 1 minute (12 213 frames). Background was corrected from each frame individually in each movie by averaging the 214 pixel intensity value of 4 background regions and subtracting this value from the mean pixel 215 intensity of the uncorrected frame (NIH ImageJ, FIJI build). Fluo-4 responses were standardized 216 for each run as fold-change from the initial frame (set to 1.0).

217

### 218 Live $Ca^{2+}$ imaging with GCaMP6f

219 At time of seeding, DRG cultures were infected with HSV-hEF1-GCaMP6f (Massachusetts 220 Institute of Technology Viral Core Facility) followed by 24 hours to allow for neurite growth 221 and GCaMP6f expression. Images of NGF-supplied or deprived axons were acquired at a rate of 222 one every 10 minutes on a Zeiss ObserverZ.1 inverted epifluorescence microscope. Multiple 223 field positions were imaged with an automated stage and atmosphere-controlled incubation 224 chamber (Pecon) controlled by ZEN2 software, and 40x objective using a 470 nm Colibri LED 225 light source (Zeiss). Axons were cropped from these movies and background was corrected on 226 each frame using ImageJ (FIJI build, NIH) by averaging background regions immediately 227 adjacent to either side of the axon and subtracting this value from each pixel of the uncorrected 228 frame. To standardize fluorescence intensity to the time of morphological degeneration, the 229 frame where axon collapse accompanied by membrane spheroids was observed was considered 230 time = 0, and time-course values were then standardized to the corrected intensity value of the 231 frame acquired 180 minutes prior and expressed as fold-change from 1.0.

232

### 233 Experimental Design and Statistical Analysis

Data was plotted and analyzed with Prism 6 (GraphPad). One-factor ANOVA with Dunnett's post-hoc comparisons were used to analyze the effects of capsazepine, NAC, VAS2870, Go6976 and Go6983 on Fluo-4 intensity standardized to the mean NGF control value, the effect of capsazepine on axon density after NGF deprivation versus the NGF-deprived control, and the effect of NGF deprivation on GCaMP6f response (RM in the 'time' factor, . Two-factor ANOVA was utilized to test the effect of EDTA on axon density (RM in the 'distance from 240 soma' factor and Dunnett's post-hoc comparisons with NGF-deprived control) and the effect of 241 NAC, VAS2870, Go6976 and Go6983 on axon density (Tukey's post-hoc comparisons and RM 242 in the 'distance from soma' factor). Two-factor ANOVA was also used to analyze the effect of 243 TrpV1 knockout on axon density after NGF deprivation and to assess the effect of capsazepine 244 on maximum Fluo-4 response to PMA (Tukey's post-hoc comparisons made in each case). A 245 two-way ANOVA (RM in the time factor) with Sidak's multiple comparisons was performed on 246 data collected during time-course imaging of the Fluo-4 response to PMA in wild-type and 247 TrpV1-null axons. Unpaired, two-tailed t-tests were used to test the significance of the Fluo-4 248 response to PMA and NGF deprivation and to test the effect of TrpV1 knockout on PMA 249 responses. Plotted values in each case represent the mean of a single embryo, and the number of 250 embryos n in each experiment and condition is described in corresponding figure legends. Full 251 statistical results are available upon request.

252

### 253 Table 1. Materials list

Reagent	Source	Identifier
Antibodies		
Mouse anti-tubulin beta III	EMD Millipore	MAB5564
Goat anti-mouse AlexaFluor 488	Jackson ImmunoResearch	115-545-003
Goat anti-mouse HRP	Jackson ImmunoResearch	115-053-146
Mice		
CD1	Charles River	IMSR Cat# CRL:22, RRID:IMSR CRL:22
B6.129X1-Trpv1 <sup>tm1Jul</sup> /J	The Jackson Laboratories	3834761, RRID:MGI:3834761
Software		

Prism 6	GraphPad	RRID:SCR_002798
Inkscape 0.91	The Inkscape	RRID:SCR_014479
	Project	
FIJI	NIH	RRID:SCR_002285
Axoquant2.0	(Johnstone et al., 2018)	http://www.github.com/BarkerLabUBC
RStudio 1.1.442	RStudio	RRID:SCR_000432
ZEN 2	Zeiss	RRID:SCR_013672
LAS X	Leica	RRID:SCR_013673
Culture reagents		
Neurobasal	Gibco	21103049
B-27	Gibco	17504-044
Penicillin/streptomycin	Gibco	15140122
GlutaMax	Gibco	35050-061
NGF	CedarLane	CLMCNET-001
Poly-D-Lysine	Sigma	P6407-5MG
Laminin/Entactin	Corning	08-774-555
Collagen	PurCol	5005-100ML
Oligonucleotides		
For <i>TrpV1</i> genotyping (wild- type forward) TGGCTCATATTTGCCTTCA G	Invitrogen	19922
For <i>TrpV1</i> genotyping (mutant forward) TAAAGCGCATGCTCCAGAC T	Invitrogen	oIMR1627

For TrpV1 genotyping (in-	Invitrogen	19923
common reverse)		
CAGCCCTAGGAGTTGATGG		
А		

### 256 **Results**

### 257 $Ca^{2+}$ influx is required for axon degeneration

We previously showed that chelation of extracellular Ca<sup>2+</sup> by EGTA rescues axons from trophic 258 259 withdrawal-induced degeneration (Johnstone et al., 2018). To confirm that NGF deprivation induces an increase in axoplasmic Ca<sup>2+</sup>, DRG axons were withdrawn from NGF and examined 260 by Ca<sup>2+</sup> imaging using the dark-to-bright Ca<sup>2+</sup>-responsive dye fluo-4. Figure 1A-B shows that 261 axoplasmic Ca<sup>2+</sup> is significantly increased at 15 hours of NGF withdrawal. To understand the 262 kinetics of the Ca<sup>2+</sup> increase relative to the timing of membrane spheroid formation and frank 263 264 degeneration, axons were infected with herpes simplex virus (HSV) harbouring the geneticallyencoded Ca2+ sensor GCaMP6f and live-imaged after NGF deprivation to record the timing of 265  $Ca^{2+}$  rise (Figure 1C). Because the degeneration of individual axons is not perfectly 266 267 synchronized, videos were standardized to the frame in which axons acquired membrane 268 spheroids; this approach revealed that an increase in the GCaMP6f signal is initiated 269 approximately two hours pror to morphological degeneration and peaks in the last 40 minutes prior to frank axon breakdown (Figure 1D). Thus, the Ca<sup>2+</sup> influx occurs prior to the emergence 270 271 of gross morphological changes.

Since NGF deprivation induced a significant axoplasmic  $Ca^{2+}$  influx proximal to membrane spheroid formation, and we recently reported that  $Ca^{2+}$  chelation rescues axons from degeneration (Johnstone et al., 2018), we sought to clarify whether  $Ca^{2+}$  signaling is required during the early phase after NGF deprivation to induce degeneration, or whether  $Ca^{2+}$  is only required as a late event. DRG neurons were grown in NGF and then either maintained in NGF, deprived of NGF or deprived of NGF in the presence of EDTA added at the beginning of the deprivation phase (EDTA 24 hours) or only after the first 12 hours of deprivation (Figure 1E).

Axon density vs distance was quantified using Axoquant2.0 (Figure 1F). Axons were rescued from degeneration when EDTA was added for the full 24 hours of NGF withdrawal or when added for the final 12 hours (Figure 1G). Intrigingly, axons were more robustly protected when EDTA was added only for the final 12 hours of NGF deprivation, versus deprived axons continuously supplied with EDTA for the entire 24-hour deprivation period, likely indicative of the important role for  $Ca^{2+}$  in outgrowth and survival pathways. We conclude that  $Ca^{2+}$  influx is a late event in axonal degeneration induced by NGF withdrawal.

286

### 287 TRPV1 mediates developmental degeneration

Capsaicin-induced activation of TRPV1 can induce Ca<sup>2+</sup>-dependent degeneration of sensory 288 289 nerve fibres (Jancso et al., 1985; Gibbons et al., 2010; Chiang et al., 2015; Savk, 2016) but to 290 date, the role for TRPV1 in developmental degeneration has not been explored. To address this, 291 we deprived DRG sensory neurons of NGF in the presence or absence of TRPV1 antagonist capsazepine and measured axonal  $Ca^{2+}$  levels using fluo-4. Figure 2A shows that the increase in 292 axonal Ca<sup>2+</sup> concentration that normally occurs following NGF deprivation was lost in the 293 294 presence of the TRPV1 inhibitor (quantified in Figure 2B). Further, the fragmentation of the 295 axonal tubulin cytoskeleton that is normally observed after 24 hours of NGF deprivation was substantially reduced in axons treated with capsazepine (Figure 2C and 2D) as well as in TRPV1 296 <sup>/-</sup> DRG axons (Figure 2E). We conclude that TRPV1-dependent Ca<sup>2+</sup> entry plays an important 297 298 role in developmental sensory axon degeneration.

299

300 ROS generated by NOX complexes are required for degeneration

ROS are important physiological regulators of TRPV1 (Salazar et al., 2008a; Ding et al., 2016; Hargreaves and Ruparel, 2016; Ogawa et al., 2016). To explore the possibility that ROS are generated following NGF deprivation, we first asked if the rise in axonal Ca<sup>2+</sup> that occurs after NGF deprivation is blocked in the presence of N-acetylcysteine (NAC), a potent antioxidant. Figure 3A and 3B show that NAC completely blocked the rise in axonal Ca<sup>2+</sup> influx that normally occurs 15 hours after NGF deprivation.

307 Under normal physiological circumstances, a major source of intracellular ROS are NOX 308 complexes (Li et al., 2006; Cao et al., 2007; Ibi et al., 2008; Kallenborn-Gerhardt et al., 2014; 309 Spencer and Engelhardt, 2014). To determine if NOX complex activity contributes to the axonal Ca<sup>2+</sup> influx that occurs in DRG sensory axons after NGF withdrawal, we exposed axons to NOX 310 complex inhibitor VAS2870. Figures 3A and 3B show that VAS2870 blocks the Ca<sup>2+</sup> influx that 311 312 normally occurs 15 hours after NGF deprivation. Both NAC and VAS2870 rescue axons from 313 degeneration following NGF withdrawal (Figures 3 C-E). Axon protection was also conferred by 314 two additional NOX complex inhibitors besides VAS2870, apocynin and diphenyliodonium 315 (data not shown). Therefore, we conclude that NOX-dependent ROS generation plays a critical 316 role in developmental axon degeneration.

317

In several settings, NOX complexes are activated by PKC (Frey et al., 2002; Ibi et al., 2008; Cosentino-Gomes et al., 2012) and we therefore asked if PKC activity mediates  $Ca^{2+}$  entry and developmental sensory axon degeneration. First, we performed gain of function experiments to determine whether PKC activation is sufficient to drive  $Ca^{2+}$  influx by exposing axons to phorbol 12-myristate 13-acetate (PMA), a potent PKC activator. Figures 4A and 4B show that PMAmediated PKC stimulation potently induces  $Ca^{2+}$  influx in axons Next, we applied PKC inhibitors to axons during NGF deprivation. Figures 4C and 4D show that PKC inhibitors Gö6976 and Gö6983 each strongly blocked the Ca<sup>2+</sup> influx induced by 15 hours of NGF deprivation and Figures 4E and 4F show that these compounds significantly improve axon integrity observed after 24 hours of NGF deprivation. These results are consistent with the hypothesis that PKC-dependent NOX activation drives TRPV1 opening following NGF deprivation.

330

To determine if any of this PKC-dependent Ca<sup>2+</sup> influx occurred via TRPV1, axons were 331 332 exposed to PMA in the absence and presence of capsazepine. Interestingly, the TRPV1 blocker capsazepine strongly reduced the PMA-induced Ca<sup>2+</sup> entry into axons, suggesting that PKC 333 mediates Ca<sup>2+</sup> entry into sensory axons mainly via TRPV1 (Figure 5A-C). To confirm this, we 334 examined the effect of PMA on Ca<sup>2+</sup> entry in DRG sensory axons derived from wild-type and 335 TRPV1<sup>-/-</sup> embryos; Figure 5D and 5E show that the PMA-induced Ca<sup>2+</sup> influx that occurs in 336 wild-type axons is virtually absent in TRPV1<sup>-/-</sup> axons. Together these results suggest that TRPV1 337 is the predominant Ca<sup>2+</sup> channel activated by PKC in sensory axons. 338

339

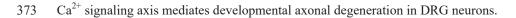
In our final experiments, we asked whether PKC-dependent TRPV1 channel activity requires NOX activation and ROS generation. Axons were exposed to PMA in the absence and presence of apocynin (to inhibit NOX complexes) or NAC (a ROS scavenger) and assessed for  $Ca^{2+}$  entry. Figure 6 shows that both apocynin (Figure 6A and 6B) and NAC (Figure 6C and 6D) suppress PMA-induced  $Ca^{2+}$  entry. Taken together, our data indicate that a direct PKC > NOX > ROS signaling cascade activates TRPV1 in sensory axons and that this cascade plays a critical role in the developmental axon degeneration of DRG sensory axons.

### 349 Discussion

350 Axon terminals innervating the skin can be induced to degenerate by clinical application of capsaicin, an exogenous TRPV1 agonist, which activates Ca2+ influx upstream of 351 352 mitochondrial dysfunction and cytoskeletal degeneration, indicating that the molecular machinery is present within DRG axons to execute TRPV1-dependent neurite degeneration 353 (Jancso et al., 1985; Gibbons et al., 2010; Chiang et al., 2015). The Ca<sup>2+</sup>-dependent apoptotic 354 355 death of retinal ganglia cells, a neuronal subtype, subjected to experimental glaucoma in vitro 356 was also found to require TRPV1, as did apoptosis of cortical neurons exposed to 357 oxygen/glucose deprivation (Shirakawa et al., 2008; Sappington et al., 2009). We recently reported that cytoskeletal fragmentation of DRG axons is rescued by the Ca<sup>2+</sup>-specific chelator 358 EGTA during NGF deprivation in vitro, highlighting a key role for Ca<sup>2+</sup> in developmental 359 360 degeneration and prompting the current study to understand its source and regulation (Johnstone 361 et al., 2018). NGF withdrawal resulted in formation of spheroid membrane protrusions on axons 362 characteristic of apoptotic-like decoupling of membrane from underlying cytoskeletal structural support, accompanied by elevated axoplasmic free Ca<sup>2+</sup> concentration. 363

364

In the present study, we found that the rise of  $Ca^{2+}$  occurred prior to the appearance of membrane spheroids and degeneration of the axon, indicating a late role for  $Ca^{2+}$  in axon degeneration induced by NGF deprivation. Cultures of DRG deprived of NGF were rescued from  $Ca^{2+}$  influx by TRPV1 antagonist capsazepine, and pharmacological and genetic TRPV1 loss-of-function rescued cytoskeletal integrity. We hypothesized that ROS promote developmental degeneration upstream of TRPV1 and  $Ca^{2+}$  influx during trophic withdrawal. Consistent with this, antioxidant NAC rescued axons from  $Ca^{2+}$  influx and from degeneration, as did NOX complex and PKC



374

### 375 Reactive oxygen species mediate developmental degeneration

376 We sought to place TRPV1 in a signaling context downstream of NGF withdrawal by identifying 377 its mode of regulation. Though TRPV1 is activated by diverse stimuli including protons, heat, 378 lipids and plant and invertebrate defense compounds, we hypothesized that ROS are required for 379 activation of TRPV1 in the context of developmental degeneration for several reasons: 1) intraneuronal Ca2+ tone and elevated oxidative status are mutually enhancing in diverse 380 physiological settings and in disease states (Liu et al., 2003; Mattson, 2007; Bezprozvanny, 381 382 2009; Marambaud et al., 2009; Tan et al., 2011; Deheshi et al., 2015; Schampel and Kuerten, 2017; Carrasco et al., 2018); 2) ROS are crucial for TRPV1-mediated Ca2+ dynamics in 383 384 nociception and inflammation, two paradigms in which TRPV1 has been extensively studied 385 (Salazar et al., 2008b; Chuang and Lin, 2009; Wang and Chuang, 2011; Ding et al., 2016; 386 Hargreaves and Ruparel, 2016; Ogawa et al., 2016); 3) cultured sympathetic neurons and PC12 387 cells, which like DRG both require NGF for outgrowth and survival, can be rescued from neurite 388 degeneration and death by an antioxidant (Ferrari et al., 1995), and 4) redox regulation of 389 TRPV1 is well established, and intracellular redox-active cysteine residues that are targeted 390 within TRPV1 have been identified (Ibi et al., 2008; Salazar et al., 2008b; Lin et al., 2015; Ding 391 et al., 2016; Morales-Lázaro et al., 2016; Nazıroğlu, 2017). Based on these findings, we 392 hypothesized that NGF deprivation results in ROS generation that is required for the TRPV1-393 mediated Ca<sup>2+</sup> influx in DRG axons and our results clearly demonstrate this to be the case.

### 395 NOX complexes generate ROS during trophic factor deprivation

396 What is the origin of ROS in an NGF-deprived sensory axon? NOX complexes are a family of 397 membrane-associated oxidases that generate superoxide via electron transfer from NADPH that 398 participate in redox regulation of downstream targets (Frey et al., 2002; Geiszt et al., 2003; 399 Hilburger et al., 2005; Cao et al., 2009; Petry et al., 2010). In embryonic sympathetic neurons, 400 which like DRG depend on NGF for survival, genetic deletion of NOX isoform NOX2 rescued 401 axons from degeneration, as did pharmacological NOX complex inhibition (Tammariello et al., 402 2000; Hilburger et al., 2005). Further, a growing body of literature points to an intimate link 403 between NOX complex activation and TRPV1-mediated Ca<sup>2+</sup> dynamics in pain and inflammation paradigms (Ibi et al., 2008; Lin et al., 2015; Ding et al., 2016; Nazıroğlu, 2017). It 404 405 is firmly established that ROS are generated as a consequence of mitochondrial dysfunction 406 during neurite degeneration and apoptosis, and it is likely that mitochondria-derived ROS are 407 generated as axons degenerate (Hajnóczky et al.; Kirkland et al., 2002; Kirkland and Franklin, 408 2003; Celsi et al., 2009; Prudent et al., 2015). However, in DRG axons stimulated to degenerate 409 with capsaicin, loss of mitochondrial membrane potential is a consequence, not a cause, of TRPV1-mediated Ca<sup>2+</sup> influx (Czeh et al., 2005; Chiang et al., 2015). Since NOX complex 410 inhibition rescued axons from Ca<sup>2+</sup> influx and degeneration in our setting, we conclude that 411 412 NOX complexes are the primary source of ROS that contributes to TRPV1 activation in 413 degenerating axons.

414

### 415 $A PKC > NOX > ROS > TRPV1 > Ca^{2+}$ signaling cascade mediates $Ca^{2+}$ influx in DRG axons.

PKC-dependent phosphorylation of the core activator subunit p47<sup>phox</sup> plays a critical role in the
assembly and activation of several NOX complexes (El-Benna et al., 2008). Typical PKCs are

activated by Ca<sup>2+</sup> and diacylglycerol (DAG) and the pharmacological DAG mimetic PMA is a 418 419 potent PKC activator (Grimes et al., 1996; Frey et al., 2002; Ibi et al., 2008; Cosentino-Gomes et 420 al., 2012; Lucke-Wold et al., 2015). Our finding that TRPVI genetic knockout completely ablated the axonal Ca<sup>2+</sup> influx response to PMA is consistent with published in vivo data 421 422 indicating that the noxious effect of intraplantar PMA injection was mediated by TRPV1 423 (Bölcskei et al., 2005). Further, our evidence for axonal signaling cassette comprised of PKC > NOX > ROS > TRPV1 >  $Ca^{2+}$  is consistent with data from other settings (e.g. inflammation) 424 that have linked extracellular signaling to TRPV1 activation (Ibi et al., 2008; Lin et al., 2015; 425 426 Ding et al., 2016; Nazıroğlu, 2017).

427

428 *How does TrkA transduce a prodegenerative signal to the* PKC/NOX/TRPV1 *signaling* 429 *cassette?* 

The apical molecular events that link NGF deprivation to PKC activation remain unknown. In 430 431 this regard, it is notable that whereas NGF-bound TrkA activates pro-survival signaling (together with the p75 neurotrophin receptor (p75<sup>NTR</sup>), recent studies have suggested that when withdrawn 432 433 from ligand, TrkA can actually drive pro-degenerative pathways (Barker and Shooter, 1994; 434 Nikoletopoulou et al., 2010; Feinberg et al., 2017). One of the signaling events activated by 435 TrkA is the phospholipase C gamma (PLC $\chi$ ) pathway and in subsequent studies it will be 436 interesting to determine if TrkA-dependent PLCy activity plays a role in PKC activation after 437 NGF withdrawal. This intriguing possibility would be consistent with results from Calissano and colleagues that show that in NGF-treated hippocampal neurons, TrkA and PLCy phosphorylation 438 439 is rapidly lost after NGF withdrawal but both rise several hours later (Matrone et al., 2009). 440 Recent work has indicated a role for TNFR-family member death receptor 6 (DR6) in

developmental degeneration downstream of NGF deprivation (Nikolaev et al., 2009); whether
DR6 enhances PKC activation in this context is not yet known.

443

In closing, we have established a novel role for TRPV1 in developmental sensory axon degeneration and established the existence of a PKC > NOX > ROS > TRPV1 > Ca<sup>2+</sup> signaling cassette in this setting. These studies have been limited to peripheral sensory axons but TRPV1 is broadly expressed in the central nervous system, and sporadic evidence has suggested a role for TRPV1 in synapse remodeling (Ramírez-Barrantes et al., 2016). Future studies should test the intriguing possibility that selective pruning of neurites is accomplished by locally-restricted TRPV1 activation, not only in the periphery but also in the brain.

451

- 452
- 453
- 454
- 455
- 456

457

458

459

460

### References

463	
464	Barde YA (1989) Trophic factors and neuronal survival. Neuron 2:1525–1534 Available at:
465	http://www.ncbi.nlm.nih.gov/pubmed/2697237 [Accessed March 14, 2018].
466	Barker PA, Shooter EM (1994) Disruption of NGF binding to the low affinity neurotrophin
467	receptor p75LNTR reduces NGF binding to TrkA on PC12 cells. Neuron 13:203-215
468	Available at: http://www.ncbi.nlm.nih.gov/pubmed/7519025 [Accessed March 14, 2018].
469	Bedard K, Krause K-H (2007) The NOX family of ROS-generating NADPH oxidases:
470	physiology and pathophysiology. Physiol Rev 87:245–313 Available at:
471	http://www.ncbi.nlm.nih.gov/pubmed/17237347 [Accessed September 20, 2014].
472	Bezprozvanny I (2009) Calcium signaling and neurodegenerative diseases. Trends Mol Med
473	15:89-100 Available at: http://www.ncbi.nlm.nih.gov/pubmed/19230774 [Accessed March
474	16, 2018].
475	Bölcskei K, Helyes Z, Szabó Á, Sándor K, Elekes K, Németh J, Almási R, Pintér E, Petho G,
476	Szolcsányi J (2005) Investigation of the role of TRPV1 receptors in acute and chronic
477	nociceptive processes using gene-deficient mice. Pain 117:368-376 Available at:
478	www.elsevier.com/locate/pain [Accessed September 27, 2018].
479	Cao X, Dai X, Parker LM, Kreulen DL (2007) Differential regulation of NADPH oxidase in
480	sympathetic and sensory Ganglia in deoxycorticosterone acetate salt hypertension.
481	Hypertension 50:663-671 Available at: http://www.ncbi.nlm.nih.gov/pubmed/17698723
482	[Accessed October 20, 2014].
483	Cao X, Demel SL, Quinn MT, Galligan JJ, Kreulen D (2009) Localization of NADPH oxidase in
484	sympathetic and sensory ganglion neurons and perivascular nerve fibers. Auton Neurosci
485	151:90–97 Available at:
486	http://www.pubmedcentral.nih.gov/articlerender.fcgi?artid=2783262&tool=pmcentrez&ren
487	dertype=abstract [Accessed October 20, 2014].
488	Carrasco C, Naziroğlu M, Rodríguez AB, Pariente JA (2018) Neuropathic Pain: Delving into the
489	Oxidative Origin and the Possible Implication of Transient Receptor Potential Channels.
490	Front Physiol 9:95 Available at: http://www.ncbi.nlm.nih.gov/pubmed/29491840 [Accessed
491	March 26, 2018].
492	Celsi F, Pizzo P, Brini M, Leo S, Fotino C, Pinton P, Rizzuto R (2009) Mitochondria, calcium
493	and cell death: A deadly triad in neurodegeneration. Biochim Biophys Acta - Bioenerg
494	1787:335–344 Available at:
495	https://www.sciencedirect.com/science/article/pii/S0005272809000826 [Accessed March
496	16, 2018].
497	Chiang H, Ohno N, Hsieh Y-L, Mahad DJ, Kikuchi S, Komuro H, Hsieh S-T, Trapp BD (2015)
498	Mitochondrial fission augments capsaicin-induced axonal degeneration. Acta Neuropathol
499	129:81–96 Available at: http://www.ncbi.nlm.nih.gov/pubmed/25322817 [Accessed March
500	16, 2018].
501	Chuang H, Lin S (2009) Oxidative challenges sensitize the capsaicin receptor by covalent
502	cysteine modification. Proc Natl Acad Sci U S A 106:20097–20102 Available at:
503	http://www.ncbi.nlm.nih.gov/pubmed/19897733 [Accessed March 16, 2018].
504	Cosentino-Gomes D, Rocco-Machado N, Meyer-Fernandes JR (2012) Cell signaling through
505	protein kinase C oxidation and activation. Int J Mol Sci 13:10697–10721 Available at:
506	http://www.ncbi.nlm.nih.gov/pubmed/23109817 [Accessed April 1, 2018].

	507	Cox JA, Jeng AY, Sharkey NA, Blumberg PM, Tauber AI (1985) Activation of the human
	508	neutrophil nicotinamide adenine dinucleotide phosphate (NADPH)-oxidase by protein
	509	kinase C. J Clin Invest 76:1932–1938 Available at:
	510	http://www.ncbi.nlm.nih.gov/pubmed/2997297 [Accessed March 16, 2018].
	511	Czeh G, Varga A, Sandor Z, Szolcsanyi J (2005) Capsaicin-Induced Changes in the Cytosolic
	512	Calcium Level and Mitochondrial Membrane Potential. Neurophysiology 37:76-87
1	513	Available at: http://link.springer.com/10.1007/s11062-005-0048-9 [Accessed February 4,
	514	2016].
	515	Deheshi S, Dabiri B, Fan S, Tsang M, Rintoul GL (2015) Changes in mitochondrial morphology
	516	induced by calcium or rotenone in primary astrocytes occur predominantly through ros-
	517	mediated remodeling. J Neurochem.
	518	Ding R, Jiang H, Sun B, Wu X, Li W, Zhu S, Liao C, Zhong Z, Chen J (2016) Advanced
	519	oxidation protein products sensitized the transient receptor potential vanilloid 1 via NADPH
	520	oxidase 1 and 4 to cause mechanical hyperalgesia. Redox Biol 10:1–11 Available at:
	521	http://www.ncbi.nlm.nih.gov/pubmed/27665186 [Accessed March 16, 2018].
	522	El-Benna J, Dang PM-C, Gougerot-Pocidalo M-A (2008) Priming of the neutrophil NADPH
	523	oxidase activation: role of p47phox phosphorylation and NOX2 mobilization to the plasma
	524	membrane. Semin Immunopathol 30:279–289 Available at:
)	525	http://www.ncbi.nlm.nih.gov/pubmed/18536919 [Accessed November 10, 2014].
•	526	Feinberg K, Kolaj A, Wu C, Grinshtein N, Krieger JR, Moran MF, Rubin LL, Miller FD, Kaplan
	527	DR (2017) A neuroprotective agent that inactivates prodegenerative TrkA and preserves
	528	mitochondria. J Cell Biol 216:3655–3675 Available at:
	529	http://www.ncbi.nlm.nih.gov/pubmed/28877995 [Accessed October 22, 2018].
	530	Fenwick AJ, Fowler DK, Wu S-W, Shaffer FJ, Lindberg JEM, Kinch DC, Peters JH (2017)
1	531	Direct Anandamide Activation of TRPV1 Produces Divergent Calcium and Current
2	532	Responses. Front Mol Neurosci 10:200 Available at:
)	533	http://www.ncbi.nlm.nih.gov/pubmed/28680392 [Accessed March 14, 2018].
	534	Ferrari G, Yan CY, Greene LA (1995) N-acetylcysteine (D- and L-stereoisomers) prevents
-	535	apoptotic death of neuronal cells. J Neurosci 15:2857–2866 Available at:
)	536	http://www.ncbi.nlm.nih.gov/pubmed/7722634 [Accessed November 5, 2014].
١.	537	Fischer LR, Glass JD (2007) Axonal degeneration in motor neuron disease. Neurodegener Dis
	538	4:431–442 Available at: http://www.ncbi.nlm.nih.gov/pubmed/17934327 [Accessed
	539	October 29, 2014].
•	540	Frey RS, Rahman A, Kefer JC, Minshall RD, Malik AB (2002) PKCzeta regulates TNF-alpha-
	541	induced activation of NADPH oxidase in endothelial cells. Circ Res 90:1012-1019
	542	Available at: http://www.ncbi.nlm.nih.gov/pubmed/12016268 [Accessed November 10,
)	543	2014].
	544	Geiszt M, Lekstrom K, Witta J, Leto TL (2003) Proteins homologous to p47phox and p67phox
	545	support superoxide production by NAD(P)H oxidase 1 in colon epithelial cells. J Biol Chem
	546	278:20006–20012 Available at:
1	547	http://www.jbc.org/content/278/22/20006?ijkey=91d5f6e627439953162c9dbb6190b7cb29e
	548	e6142&keytype2=tf_ipsecsha [Accessed November 8, 2014].
7	549	Geron M, Hazan A, Priel A (2017) Animal Toxins Providing Insights into TRPV1 Activation
	550	Mechanism. Toxins (Basel) 9:326 Available at:
	551	http://www.ncbi.nlm.nih.gov/pubmed/29035314 [Accessed March 14, 2018].
	552	Gibbons CH, Wang N, Freeman R (2010) Capsaicin induces degeneration of cutaneous

552	
553	autonomic nerve fibers. Ann Neurol 68:888–898 Available at:
554	http://www.ncbi.nlm.nih.gov/pubmed/21061393 [Accessed March 16, 2018].
555	Grabiec U, Dehghani F (2017) N - Arachidonoyl Dopamine: A Novel Endocannabinoid and
556	Endovanilloid with Widespread Physiological and Pharmacological Activities. Cannabis
557	Cannabinoid Res 2:183–196 Available at: http://www.ncbi.nlm.nih.gov/pubmed/29082315
558	[Accessed March 14, 2018].
559	Grimes ML, Zhou J, Beattie EC, Yuen EC, Hall DE, Valletta JS, Topp KS, LaVail JH, Bunnett
560	NW, Mobley WC (1996) Endocytosis of activated TrkA: evidence that nerve growth factor
561	induces formation of signaling endosomes. J Neurosci 16:7950–7964 Available at:
562	http://www.ncbi.nlm.nih.gov/pubmed/8987823 [Accessed November 9, 2014].
563	Hajnóczky G, Csordás G, Das S, Garcia-Perez C, Saotome M, Sinha Roy S, Yi M Mitochondrial
564	calcium signalling and cell death: approaches for assessing the role of mitochondrial Ca2+
565	uptake in apoptosis. Cell Calcium 40:553–560 Available at:
566	http://www.pubmedcentral.nih.gov/articlerender.fcgi?artid=2692319&tool=pmcentrez&ren
567	dertype=abstract [Accessed November 19, 2015].
568	Hakim M, Jiang W, Luo L, Li B, Yang S, Song Y, Lai R (2015) Scorpion Toxin, BmP01,
569	Induces Pain by Targeting TRPV1 Channel. Toxins (Basel) 7:3671–3687 Available at:
570	http://www.ncbi.nlm.nih.gov/pubmed/26389953 [Accessed March 14, 2018].
571	Hargreaves KM, Ruparel S (2016) Role of Oxidized Lipids and TRP Channels in Orofacial Pain
572	and Inflammation. J Dent Res 95:1117–1123 Available at:
573	http://www.ncbi.nlm.nih.gov/pubmed/27307050 [Accessed March 16, 2018].
574	Hilburger EW, Conte EJ, McGee DW, Tammariello SP (2005) Localization of NADPH oxidase
575	subunits in neonatal sympathetic neurons. Neurosci Lett 377:16-19 Available at:
576	http://www.ncbi.nlm.nih.gov/pubmed/15722179 [Accessed October 20, 2014].
577	Ibi M, Matsuno K, Shiba D, Katsuyama M, Iwata K, Kakehi T, Nakagawa T, Sango K, Shirai Y,
578	Yokoyama T, Kaneko S, Saito N, Yabe-Nishimura C (2008) Reactive oxygen species
579	derived from NOX1/NADPH oxidase enhance inflammatory pain. J Neurosci 28:9486–
580	9494 Available at: http://www.ncbi.nlm.nih.gov/pubmed/18799680 [Accessed March 15,
581	2018].
582	Jancso G, Király E, Joó F, Such G, Nagy A (1985) Selective degeneration by capsaicin of a
583	subpopulation of primary sensory neurons in the adult rat. Neurosci Lett 59:209–214
584	Available at: https://www.sciencedirect.com/science/article/pii/0304394085902010
585	[Accessed March 16, 2018].
586	Johnstone AD, Hallett RM, de Léon A, Carturan B, Gibon J, Barker PA (2018) A novel method
587	for quantifying axon degeneration Gillingwater TH, ed. PLoS One 13:e0199570 Available
588	at: http://dx.plos.org/10.1371/journal.pone.0199570 [Accessed September 5, 2018].
589	Julius D, Caterina MJ, Schumacher MA, Tominaga M, Rosen TA, Levine JD (1997) The
590	capsaicin receptor: a heat-activated ion channel in the pain pathway. Nature 389:816–824
591	Available at: http://www.ncbi.nlm.nih.gov/pubmed/9349813 [Accessed March 14, 2018].
592	Kallenborn-Gerhardt W, Hohmann SW, Syhr KMJ, Schröder K, Sisignano M, Weigert A,
593	Lorenz JE, Lu R, Brüne B, Brandes RP, Geisslinger G, Schmidtko A (2014) Nox2-
594	dependent signaling between macrophages and sensory neurons contributes to neuropathic
595	pain hypersensitivity. Pain 155:2161–2170 Available at:
596	http://www.ncbi.nlm.nih.gov/pubmed/25139590 [Accessed October 20, 2014].
597	Kanaan NM, Pigino GF, Brady ST, Lazarov O, Binder LI, Morfini GA (2013) Axonal
598	degeneration in Alzheimer's disease: when signaling abnormalities meet the axonal

599	transport system. Exp Neurol 246:44–53 Available at:
600	http://www.pubmedcentral.nih.gov/articlerender.fcgi?artid=3465504&tool=pmcentrez&ren
601	dertype=abstract [Accessed October 27, 2014].
602	Kirkland RA, Franklin JL (2003) Bax, reactive oxygen, and cytochrome c release in neuronal
603	apoptosis. Antioxid Redox Signal 5:589–596 Available at:
604	http://online.liebertpub.com/doi/abs/10.1089/152308603770310257 [Accessed November 5,
605	2014].
606	Kirkland RA, Windelborn JA, Kasprzak JM, Franklin JL (2002) A Bax-induced pro-oxidant
607	state is critical for cytochrome c release during programmed neuronal death. J Neurosci
608	22:6480-6490 Available at: http://www.ncbi.nlm.nih.gov/pubmed/12151527 [Accessed
609	November 9, 2014].
610	Li Q, Harraz MM, Zhou W, Zhang LN, Ding W, Zhang Y, Eggleston T, Yeaman C, Banfi B,
611	Engelhardt JF (2006) Nox2 and Rac1 regulate H2O2-dependent recruitment of TRAF6 to
612	endosomal interleukin-1 receptor complexes. Mol Cell Biol 26:140–154 Available at:
613	http://mcb.asm.org/content/26/1/140.long [Accessed October 22, 2014].
614	Li Q, Spencer NY, Oakley FD, Buettner GR, Engelhardt JF (2009) Endosomal Nox2 facilitates
615	redox-dependent induction of NF-kappaB by TNF-alpha. Antioxid Redox Signal 11:1249–
616	1263 Available at:
617	http://www.pubmedcentral.nih.gov/articlerender.fcgi?artid=2842115&tool=pmcentrez&ren
618	dertype=abstract [Accessed November 10, 2014].
619	Lin C-S, Lee S-H, Huang H-S, Chen Y-S, Ma M-C (2015) H 2 O 2 generated by NADPH
620	oxidase 4 contributes to transient receptor potential vanilloid 1 channel-mediated
621	mechanosensation in the rat kidney. Am J Physiol - Ren Physiol 309:F369–F376 Available
622	at: https://pdfs.semanticscholar.org/14fd/d5a7cc35aaf2c922b2b69e53c87e42d039a9.pdf
623	[Accessed March 16, 2018].
624	Liu M, Liu M-C, Magoulas C, Priestley J V, Willmott NJ (2003) Versatile regulation of
625	cytosolic Ca2+ by vanilloid receptor I in rat dorsal root ganglion neurons. J Biol Chem
626	278:5462–5472 Available at: http://www.jbc.org/content/278/7/5462.full [Accessed
627	February 4, 2016].
628	Lucke-Wold BP, Turner RC, Logsdon AF, Simpkins JW, Alkon DL, Smith KE, Chen Y-W, Tan
628 629	Z, Huber JD, Rosen CL (2015) Common mechanisms of Alzheimer's disease and ischemic
630	stroke: the role of protein kinase C in the progression of age-related neurodegeneration. J
631	Alzheimers Dis 43:711–724 Available at: http://www.ncbi.nlm.nih.gov/pubmed/25114088
632	[Accessed April 27, 2017].
633	Maher P, Schubert D (2000) Signaling by reactive oxygen species in the nervous system. Cell
634	Mol Life Sci 57:1287–1305 Available at: http://www.ncbi.nlm.nih.gov/pubmed/11028919
635	[Accessed November 10, 2014].
636	Marambaud P, Dreses-Werringloer U, Vingtdeux V (2009) Calcium signaling in
637	neurodegeneration. Mol Neurodegener 4:20 Available at:
638	http://www.ncbi.nlm.nih.gov/pubmed/19419557 [Accessed March 16, 2018].
639	Matrone C, Marolda R, Ciafrè S, Ciotti MT, Mercanti D, Calissano P (2009) Tyrosine kinase
640	nerve growth factor receptor switches from prosurvival to proapoptotic activity via Abeta-
641	mediated phosphorylation. Proc Natl Acad Sci U S A 106:11358–11363 Available at:
642	http://www.ncbi.nlm.nih.gov/pubmed/19549834 [Accessed September 21, 2018].
643	Mattson MP (2007) Calcium and neurodegeneration. Aging Cell 6:337–350 Available at:
644	http://www.ncbi.nlm.nih.gov/pubmed/17328689 [Accessed March 16, 2018].

645	Morales-Lázaro SL, Llorente I, Sierra-Ramírez F, López-Romero AE, Ortíz-Rentería M,
646	Serrano-Flores B, Simon SA, Islas LD, Rosenbaum T (2016) Inhibition of TRPV1 channels
647	by a naturally occurring omega-9 fatty acid reduces pain and itch. Nat Commun 7:13092
648	Available at: http://www.ncbi.nlm.nih.gov/pubmed/27721373 [Accessed March 16, 2018].
649	Murphy R, Acheson A, Hodges R, Haskins J, Richards C, Reklow E, Chlumecky V, Barker P,
650	Alderson R, Lindsay R (1993) Immunological relationships of NGF, BDNF, and NT-3:
651	recognition and functional inhibition by antibodies to NGF. J Neurosci 13:2853-2862.
652	Nazıroğlu M (2017) Activation of TRPM2 and TRPV1 Channels in Dorsal Root Ganglion by
653	NADPH Oxidase and Protein Kinase C Molecular Pathways: a Patch Clamp Study. J Mol
654	Neurosci 61:425-435 Available at: http://www.ncbi.nlm.nih.gov/pubmed/28097492
655	[Accessed April 1, 2018].
656	Nikolaev A, McLaughlin T, O'Leary DDM, Tessier-Lavigne M (2009) APP binds DR6 to
657	trigger axon pruning and neuron death via distinct caspases. Nature 457:981-989 Available
658	at: http://www.nature.com/nature/journal/v457/n7232/full/nature07767.html#online-
659	methods [Accessed October 27, 2014].
660	Nikoletopoulou V, Lickert H, Frade JM, Rencurel C, Giallonardo P, Zhang L, Bibel M, Barde Y-
661	A (2010) Neurotrophin receptors TrkA and TrkC cause neuronal death whereas TrkB does
662	not. Nature 467:59-63 Available at: http://dx.doi.org/10.1038/nature09336 [Accessed
663	October 19, 2014].
664	Ogawa N, Kurokawa T, Fujiwara K, Polat OK, Badr H, Takahashi N, Mori Y (2016) Functional
665	and Structural Divergence in Human TRPV1 Channel Subunits by Oxidative Cysteine
666	Modification. J Biol Chem 291:4197–4210 Available at:
667	http://www.ncbi.nlm.nih.gov/pubmed/26702055 [Accessed March 16, 2018].
668	Pal R, Basu Thakur P, Li S, Minard C, Rodney GG (2013) Real-time imaging of NADPH
669	oxidase activity in living cells using a novel fluorescent protein reporter. PLoS One
670	8:e63989 Available at:
671	http://www.pubmedcentral.nih.gov/articlerender.fcgi?artid=3660327&tool=pmcentrez&ren
672	dertype=abstract [Accessed November 7, 2014].
673	Patel TD, Jackman A, Rice FL, Kucera J, Snider WD (2000) Development of sensory neurons in
674	the absence of NGF/TrkA signaling in vivo. Neuron 25:345-357 Available at:
675	http://www.ncbi.nlm.nih.gov/pubmed/10719890 [Accessed November 9, 2014].
676	Petry A, Weitnauer M, Görlach A (2010) Receptor activation of NADPH oxidases. Antioxid
677	Redox Signal 13:467-487 Available at: http://www.ncbi.nlm.nih.gov/pubmed/20001746
678	[Accessed November 10, 2014].
679	Prudent J, Zunino R, Sugiura A, Mattie S, Shore GC, McBride HM (2015) MAPL SUMOylation
680	of Drp1 Stabilizes an ER/Mitochondrial Platform Required for Cell Death. Mol Cell
681	59:941–955 Available at: http://www.ncbi.nlm.nih.gov/pubmed/26384664 [Accessed
682	February 15, 2016].
683	Ramírez-Barrantes R, Cordova C, Poblete H, Muñoz P, Marchant I, Wianny F, Olivero P (2016)
684	Perspectives of TRPV1 Function on the Neurogenesis and Neural Plasticity. Neural Plast
685	2016:1-12 Available at: http://www.ncbi.nlm.nih.gov/pubmed/26881090 [Accessed March
686	12, 2018].
687	Reczek CR, Chandel NS (2014) ROS-dependent signal transduction. Curr Opin Cell Biol 33C:8-
688	13 Available at: http://www.ncbi.nlm.nih.gov/pubmed/25305438 [Accessed October 12,
689	2014].

690 Salazar H, Llorente I, Jara-Oseguera A, García-Villegas R, Munari M, Gordon SE, Islas LD,

1	Rosenbaum T (2008a) A single N-terminal cysteine in TRPV1 determines activation by
2	pungent compounds from onion and garlic. Nat Neurosci 11:255–261 Available at:
3	http://www.ncbi.nlm.nih.gov/pubmed/18297068 [Accessed March 15, 2018].
4	Salazar H, Llorente I, Jara-Oseguera A, García-Villegas R, Munari M, Gordon SE, Islas LD,
5	Rosenbaum T (2008b) A single N-terminal cysteine in TRPV1 determines activation by
6	pungent compounds from onion and garlic. Nat Neurosci 11:255–261 Available at:
7	http://www.nature.com/articles/nn2056 [Accessed March 16, 2018].
8	Sann H, Jancsó G, Ambrus A, Pierau F-K (1995) Capsaicin treatment induces selective sensory
9	degeneration and increased sympathetic innervation in the rat ureter. Neuroscience 67:953-
0	966 Available at: https://www.sciencedirect.com/science/article/pii/0306452295001020
1	[Accessed March 16, 2018].
2	Sappington RM, Sidorova T, Long DJ, Calkins DJ (2009) TRPV1: contribution to retinal
3	ganglion cell apoptosis and increased intracellular Ca2+ with exposure to hydrostatic
4	pressure. Invest Ophthalmol Vis Sci 50:717–728 Available at:
5	http://iovs.arvojournals.org/article.aspx?doi=10.1167/iovs.08-2321 [Accessed March 11,
6	2018].
7	Şavk E (2016) Neurologic Itch Management. In: Current problems in dermatology, pp 116–123
8	Available at: http://www.ncbi.nlm.nih.gov/pubmed/27578080 [Accessed March 16, 2018].
9	Saxena S, Caroni P (2007) Mechanisms of axon degeneration: from development to disease.
0	Prog Neurobiol 83:174–191 Available at: http://www.ncbi.nlm.nih.gov/pubmed/17822833
1	[Accessed November 6, 2014].
2	Schampel A, Kuerten S (2017) Danger: High Voltage—The Role of Voltage-Gated Calcium
3	Channels in Central Nervous System Pathology. Cells 6:43 Available at:
4	http://www.ncbi.nlm.nih.gov/pubmed/29140302 [Accessed November 29, 2017].
5	Schuldiner O, Yaron A (2014) Mechanisms of developmental neurite pruning. Cell Mol Life Sci
6	Available at: http://www.ncbi.nlm.nih.gov/pubmed/25213356 [Accessed October 24, 2014].
7	Shirakawa H, Yamaoka T, Sanpei K, Sasaoka H, Nakagawa T, Kaneko S (2008) TRPV1
8	stimulation triggers apoptotic cell death of rat cortical neurons. Biochem Biophys Res
9	Commun 377:1211–1215 Available at: http://www.ncbi.nlm.nih.gov/pubmed/18996081
0	[Accessed March 30, 2018].
1	Spencer NY, Engelhardt JF (2014) The basic biology of redoxosomes in cytokine-mediated
2	signal transduction and implications for disease-specific therapies. Biochemistry 53:1551–
3	1564 Available at: http://www.ncbi.nlm.nih.gov/pubmed/24555469 [Accessed June 27,
4	2018].
5	Tait SWG, Green DR (2010) Mitochondria and cell death: outer membrane permeabilization and
6	beyond. Nat Rev Mol Cell Biol 11:621–632 Available at:
7	http://dx.doi.org/10.1038/nrm2952 [Accessed September 20, 2015].
8	Tammariello SP, Quinn MT, Estus S (2000) NADPH oxidase contributes directly to oxidative
9	stress and apoptosis in nerve growth factor-deprived sympathetic neurons. J Neurosci
0	20:RC53 Available at: http://www.ncbi.nlm.nih.gov/pubmed/10627630 [Accessed October
1	20, 2014].
2	Tan AR, Cai AY, Deheshi S, Rintoul GL (2011) Elevated intracellular calcium causes distinct
3	mitochondrial remodelling and calcineurin-dependent fission in astrocytes. Cell Calcium
4	49:108-114 Available at: http://www.ncbi.nlm.nih.gov/pubmed/21216007 [Accessed
5	August 22, 2017].
6	Vickers JC, King AE, Woodhouse A, Kirkcaldie MT, Staal JA, McCormack GH, Blizzard CA,

737	Musgrove REJ, Mitew S, Liu Y, Chuckowree JA, Bibari O, Dickson TC (2009)
738	Axonopathy and cytoskeletal disruption in degenerative diseases of the central nervous
739	system. Brain Res Bull 80:217–223 Available at:
740	http://www.ncbi.nlm.nih.gov/pubmed/19683034 [Accessed October 31, 2014].
741	Vogelbaum MA, Tong JX, Rich KM (1998) Developmental regulation of apoptosis in dorsal
742	root ganglion neurons. J Neurosci 18:8928-8935 Available at:
743	http://www.ncbi.nlm.nih.gov/pubmed/9786998 [Accessed November 9, 2014].
744	Wang DH, Wu W, Lookingland KJ (n.d.) Degeneration of Capsaicin-Sensitive Sensory Nerves
745	Leads to Increased Salt Sensitivity Through Enhancement of Sympathoexcitatory Response.
746	Available at: http://hyper.ahajournals.org/content/hypertensionaha/37/2/440.full.pdf
747	[Accessed March 16, 2018].
748	Wang S, Chuang H-H (2011) C-terminal Dimerization Activates the Nociceptive Transduction
749	Channel Transient Receptor Potential Vanilloid 1 *. Publ JBC Pap Press Available at:
750	http://pubmedcentralcanada.ca/pmcc/articles/PMC3220497/pdf/zbc40601.pdf [Accessed
751	July 5, 2017].
752	

### 754 Figure Legends

755

### 756 Figure 1. Ca<sup>2+</sup> is required for developmental degeneration *in vitro*.

757 (A) Cultures of DRG explants were either maintained in NGF or deprived of NGF for 15 hours prior to loading with Ca<sup>2+</sup> sensor fluo-4. (B) Axons deprived of NGF displayed a significantly 758 elevated axonal Ca<sup>2+</sup> concentration (data standardized to NGF, n=16, compiled from NGF and 759 760 deprived controls; analyzed by unpaired two-tailed t-test and indicated are median, min/max and 25/75%). (C) Axoplasmic Ca<sup>2+</sup> influx reported by GCaMP6f occurred proximal to the time of 761 morphological degeneration of the axon. (D) Axoplasmic Ca2+ increase was significantly 762 elevated by 40 minutes prior to membrane spheroid formation but not earlier as compared to 763 764 intensity 180 minutes prior to spheroids (indicated are mean and SEM; one-factor ANOVA and 765 Dunnett's posthoc). (E) ßIII-tubulin staining of DRG explants treated with EDTA after 12 hours of NGF deprivation or for the entire 24 hour deprivation phase. Consistent with a late role for 766  $Ca^{2+}$  in axon degeneration, axons were significantly rescued from cytoskeletal fragmentation 767 even when Ca<sup>2+</sup> dynamics were left unmodulated by chelation during the first 12 hours of NGF 768 769 deprivation. (F) Axoquant2.0 output curves are shown with mean and SEM (n=9 embryos from 3 770 pooled litters). (G) Axon density within 1000 µm bins were analyzed by two-factor ANOVA and 771 Dunnett's post-hoc comparison and plotted with median, min/max and 25/75%. \*p<0.05, 772 \*\*\*\*p<0.0001.

773

## Figure 2. TRPV1 mediates $Ca^{2+}$ flux and cytoskeletal fragmentation during trophic factor deprivation. (A) TRPV1 inhibition by capsazepine rescued axons from $Ca^{2+}$ influx. Axons were loaded with fluo-4 after the indicated treatments and imaged by confocal microscopy. (B) 15

hours of NGF deprivation induced robust activation of Ca<sup>2+</sup> sensor fluo-4 in axons, but co-777 778 application of 10 µM capsazepine (TRPV1 inhibitor, CPZ) ablated the response as compared to 779 deprived controls (n=7 pooled experiments, one-factor ANOVA and Dunnett's post-hoc 780 comparison to the deprived condition). (C-D) NGF deprivation for 24 hours resulted in a 781 significant loss of tubulin-stained axons, but addition of 10 µM CPZ after 12 hours of trophic 782 withdrawal for the final 12 hours resulted in a rescue of axon density to a level not significantly 783 different from healthy controls (n=8 embryos in NGF and capsazepine conditions, n=7 in 784 DMSO; one-factor ANOVA and Dunnett's post-hoc comparison were performed on axon 785 density in a bin between 1000 and 1999 µm from soma. (E) TRPV1 knockout rescued axons 786 from cytoskeletal degeneration; neurons cultured from mixed-genotype litters were deprived of 787 NGF for 24 hours, after which TRPV1-null axons were significantly more dense than axons in 788 cultures derived from wild-type animals. Axon density between 1000 and 1999 µm from soma 789 was compared by two-factor ANOVA and Tukey 's post-hoc comparison. Indicated are median, min/max and 25/75% in each panel. \*p<0.05, \*\*\*p<0.001, \*\*\*\*p<0.0001. 790

791

Figure 3. ROS derived from NOX complexes activate Ca<sup>2+</sup> flux and axonal degeneration in 792 793 vitro. (A) DRG explants cultured in NGF were either maintained in NGF or withdrawn from 794 trophic factor for 15 hours before staining with fluo-4 and imaged by confocal microscopy. (B) Antioxidant NAC (20 mM) or NOX complex inhibition using VAS2870 (10 µM) significantly 795 impaired axonal  $Ca^{2+}$  influx induced by trophic factor withdrawal (n=3 pooled experiments 796 797 standardized to the NGF condition, one-factor ANOVA and Dunnett's post-hoc comparison; 798 mean and SEM are indicated. (C-E) Antioxidant or NOX complex inhibition significantly 799 rescued DRG axonal cytoskeleton (visualized with BIII-tubulin immunostaining) when added

after 12 hours of NGF deprivation for the final 12 hours. (D) Axoquant2.0 axon density output
curves with mean and SEM. (E) Axon density was analyzed within 1000 µm bins using twofactor ANOVA and Tukey's post-hoc analysis. Median, min/max and 25/75% are indicated.
\*p<0.05, \*\*p<0.01, \*\*\*\*p<0.0001.</li>

804

Figure 4. PKC mediates Ca<sup>2+</sup> flux and axonal degeneration *in vitro*. (A) Representative 805 micrographs of DRG axons loaded with fluo-4 and treated with PKC activator PMA (100 nM). 806 (B) Direct PKC stimulation by PMA is sufficient to activate axonal Ca<sup>2+</sup> influx (n=14 embryos 807 808 pooled from PMA and buffer controls and compared using an unpaired, two-tailed t-test.) (C-D) Ca<sup>2+</sup> influx activated by 15 hours of NGF deprivation is significantly rescued when PKC is 809 810 inhibited by Gö6976 and Gö6983 (10 µM; n=6 embryos each condition standardized to NGF 811 values and tested by one-factor ANOVA and Dunnett's post-hoc comparison. (E-F) PKC 812 inhibition after 12 hours rescues axons from cytoskeletal degeneration induced by 24 hours of 813 NGF deprivation. (E) Axoquant2.0 axon density output curves are presented with mean and SEM (n=9 for all conditions except n=7 for Gö6983). (F) Axon density was analyzed within 814 815 1000 µm bins using two-factor ANOVA and Tukey's post-hoc analysis. Median, min/max and 816 25/75% are indicated. \*\*\*\*p<0.0001.

817

Figure 5. TRPV1 mediates PKC-dependent axonal  $Ca^{2+}$  flux. (A) Representative images of DRG axons loaded with fluo-4 and live-imaged during stimulation with PKC activator PMA in the presence or absence of TRPV1 inhibitor CPZ (10  $\mu$ M). TRPV1 inhibition abolished the axonal Ca<sup>2+</sup> response to PKC activation. (B) Time-course of the fluo-4 responses to Ca<sup>2+</sup> influx during the 15-minute recording period (n=6, mean and SEM are indicated). (C) Maximum

responses during the recording period were analyzed using two-factor ANOVA and Tukey's post-hoc comparison; indicated are median, min/max and 25/75%. (D) The axonal Ca<sup>2+</sup> response to PKC activation was absent in axons of *TrpV1*-knockout DRG (n=6, mean and SEM are indicated and data was analyzed by two-factor ANOVA and Sidak's post-hoc comparison). (E) The maximum fluo-4 responses to axonal Ca<sup>2+</sup> were analyzed by an unpaired, two-tailed t-test and indicated are median, min/max and 25/75%. \*\*p<0.01, \*\*\*\*p<0.001, \*\*\*\*p<0.0001.

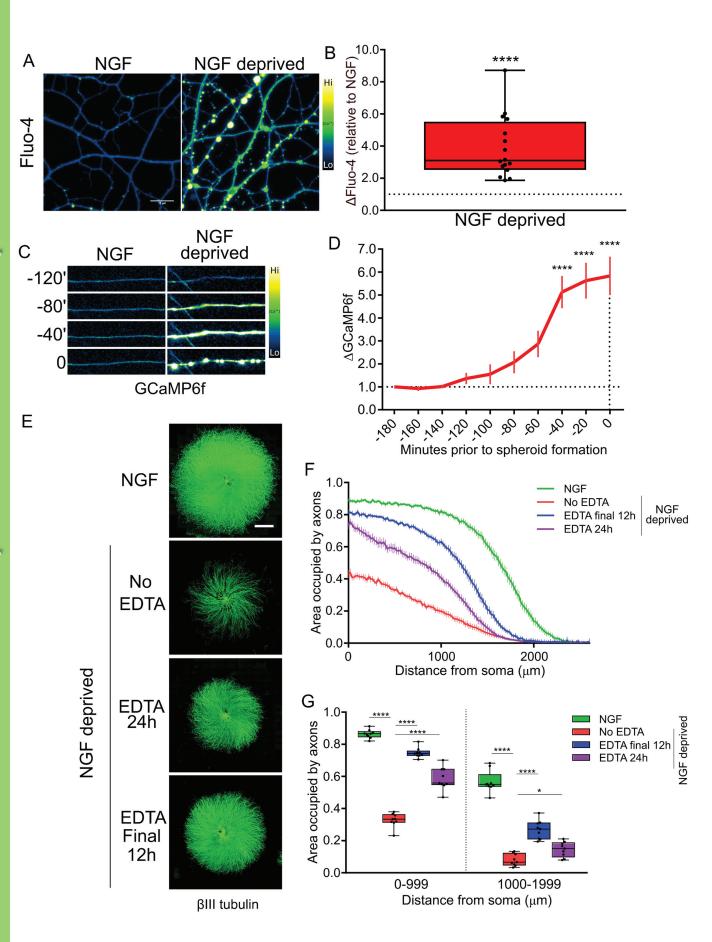
829

830

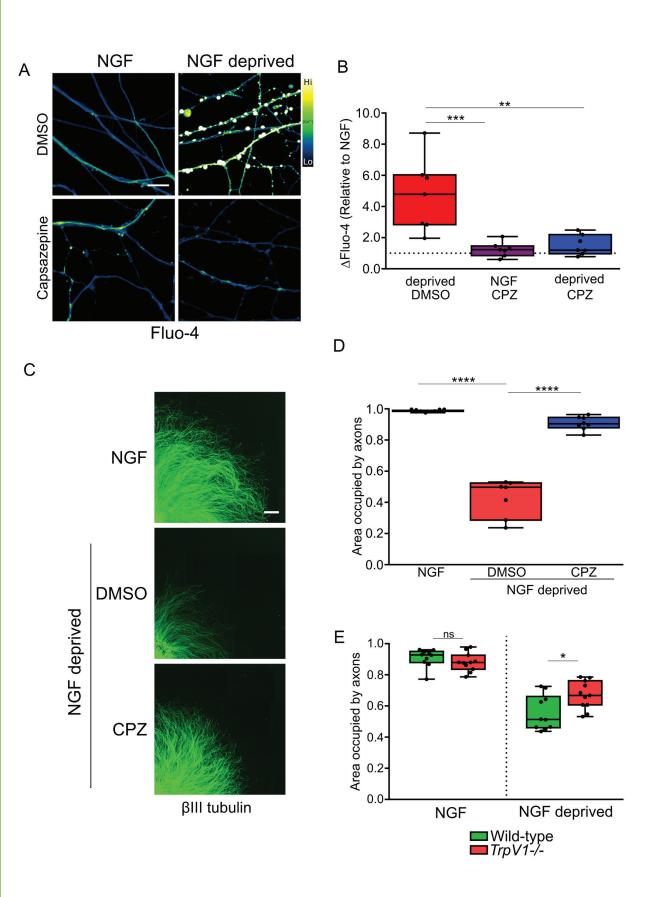
Figure 6. PKC-dependent Ca<sup>2+</sup> flux requires ROS from NOX complexes. (A) Representative 831 images of DRG axons loaded with fluo-4 and stimulated with PMA in the presence or absence of 832 apocynin (10  $\mu$ M). (B) PKC-induced Ca<sup>2+</sup> influx was significantly reduced by NOX complex 833 834 inhibition by 10 µM apocynin (n=5 pooled experiments analyzed by two-factor ANOVA and 835 Tukey's post-hoc comparison). (C) Representative images of DRG axons loaded with fluo-4 and 836 stimulated with PMA in the presence or absence of NAC (20 mM). (D) PKC activation with PMA (100 nM) induced axonal Ca<sup>2+</sup> influx that was abolished by co-application of antioxidant 837 838 NAC at 20 mM (n=6 pooled experiments analyzed by two-factor ANOVA and Tukey's post-hoc 839 comparison). Plotted are the maximum Fluo-4 responses (relative to baseline values) during the recording period. Indicated are median, min/max and 25/75%. \*p<0.05, \*\*p<0.01, \*\*\*p<0.001. 840

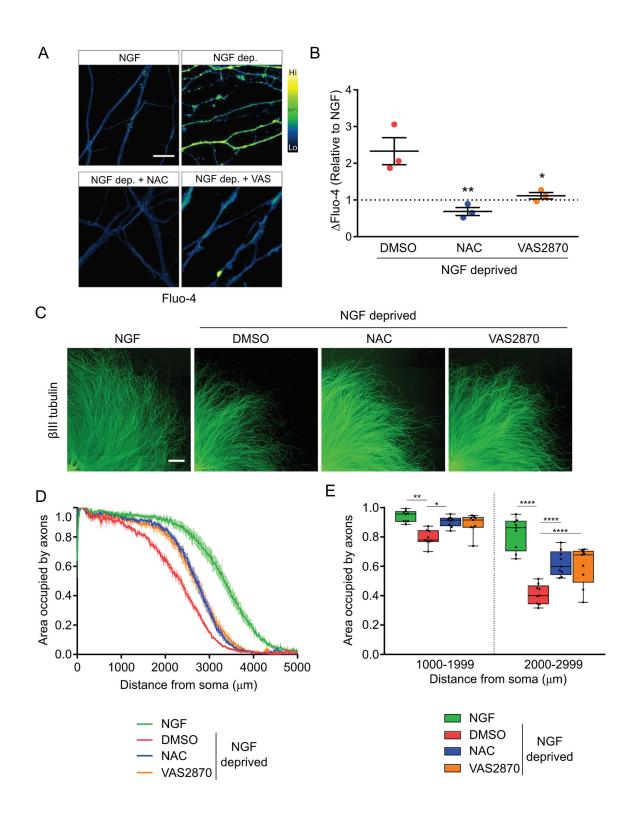
841

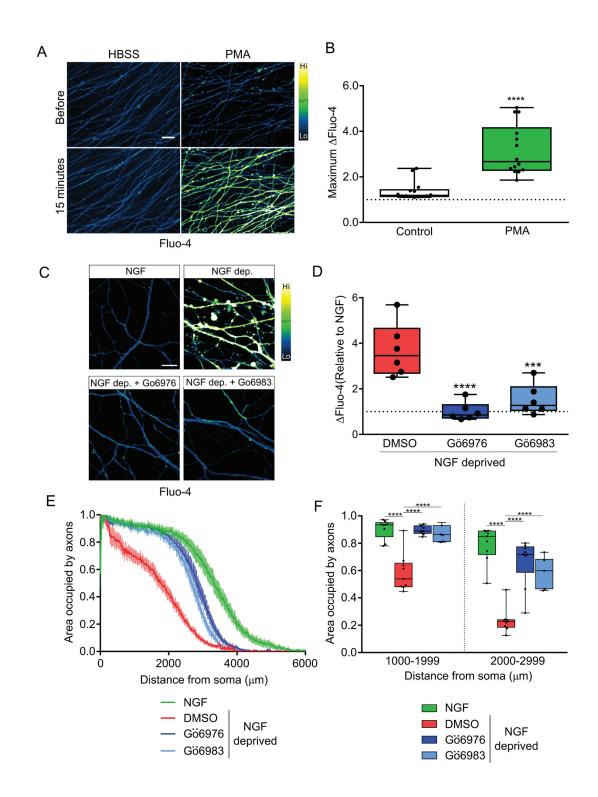
842

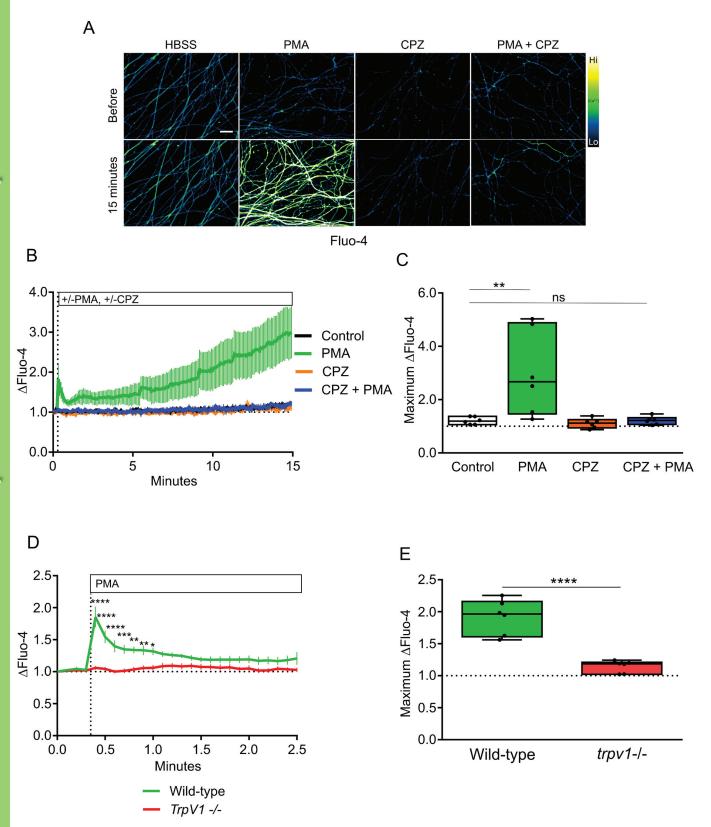




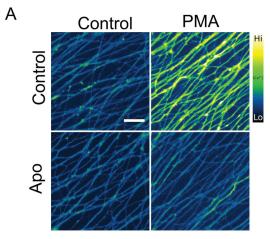






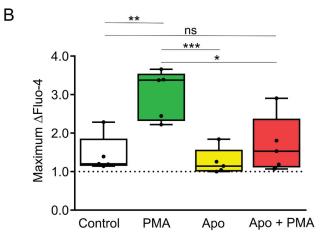


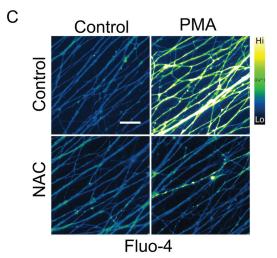




Fluo-4

D





tontrol PMA NAC NAC + PMA